Proc. Natl. Acad. Sci. USA
Vol. 92, pp. 3834–3838, April 1995
Biophysics

The photoreceptor sensory rhodopsin I as a two-photon-driven proton pump

ULRICH HAUPTS*, CHRISTINA HAUPTS, AND DIETER OESTERHELT

Max-Planck-Institut für Biochemie, Am Klopferspitz, D-82152 Martinsried, Germany

Communicated by H. Ronald Kaback, University of California, Los Angeles, CA, January 9, 1995

ABSTRACT **Proton translocation experiments with intact cells of *Halobacterium salinarium* overproducing sensory rhodopsin I (SRI) revealed transport activity of SRI in a two-photon process. The vectoriality of proton translocation depends on pH, being outwardly directed above, and inwardly directed below, pH 5.7. Activation of the transport cycle requires excitation of the initial dark state of SRI, SRI_{590}, to form the intermediate SRI_{380}. Action spectra identify the photocycle intermediates SRI_{380} and SRI_{520} as the two photochemically reactive species in the outwardly directed transport process. As shown by flash photolysis experiments, SRI_{520} undergoes a so-far unknown photochemical reaction to SRI_{380} with a half-time of <200 μs. Mutation of SRI residue Asp-76, the residue which is equivalent to the proton acceptor Asp-85 in bacteriorhodopsin, to asparagine leads to inactivation of proton translocation. This demonstrates that the underlying mechanisms of proton transport in both retinal proteins share similar features. However, SRI is to our knowledge the first case where photochemical reactions between two thermally unstable photoproducts of a retinal protein constitute a catalytic ion transport cycle.**

Four different retinal proteins have been identified in *Halobacterium salinarium*. Two of them, bacteriorhodopsin (BR) and halorhodopsin (HR), are responsible for light-energy conversion during photosynthetic growth (for recent reviews see refs. 1 and 2). The other two, sensory rhodopsin I and sensory rhodopsin II (SRI and SRII), are photoreceptors which mediate phototactic behavior of the cell (3, 4).

The absorption maximum of the dark state of SRI is pH dependent, being at 590 nm (SRI_{590}) in the acidic range and at 550 nm (SRI_{550}) in the alkaline range (5). Absorption of a photon by SRI_{590} or SRI_{550} leads to formation of the main photocycle intermediate, SRI_{380} (6). The thermal decay of SRI_{380} to the initial state has a half-time of ≈800 ms (6). Alternatively, SRI_{380} can undergo a second photoreaction yielding an intermediate with an absorption maximum at 510–530 nm. This SRI_{520} intermediate thermally decays to the initial state with a half-time of 150 ms (7). The alternative reactions allow SRI to perform dual function by mediating a photoattractant as well as a photorepellent response (8).

The SRI amino acid sequence (9) reveals a striking degree of sequence homology to BR (10) and HR (11), suggesting seven transmembrane helices (A–G) as found for BR (12) and HR (13). Retinal is bound as a protonated Schiff base (14, 15) to Lys-206 in helix G of SRI. In BR Asp-85 and Asp-96 function as proton acceptor and donor, respectively (16–18). The absence of one or both of these residues renders the proton pump inefficient for phototrophic growth, because turnover rates drop from about 100 s^{-1} to 1 s^{-1} in the case of the Asp-96 → Asn mutation, whereas in Asp-85 → Xaa mutants, M formation (deprotonation of the Schiff base) is prevented. In SRI the corresponding positions are occupied by Asp-76 and Tyr-87; i.e., the amino acid functioning as acceptor in BR is retained while the donor site is replaced by tyrosine, thus explaining the low turnover rate of the SRI photocycle. In addition, Fourier transform IR spectroscopy studies (19, 20) have shown that Asp-76 is protonated in the initial state as well as in SRI_{380}, undergoing only a change in environment during the transition. A possible ion translocation activity of SRI could not be excluded on this basis, because BR mutants lacking both donor and acceptor side chain are still active at a low level of transport rates in a two-photon process (21). However, a previous study of SRI photocycling (22) did not detect any electrogenic activity of SRI.

Until recently, experiments on SRI were carried out with wild-type cells and derived membrane fractions where SRI occurs as a stoichiometric complex with its transducer protein HtrI (23–25). The thermal decay of SRI_{380} is independent of bulk pH in the case of the HtrI–SRI complex, while an exponential increase in the decay time of SRI_{380} with increasing pH is observed for SRI alone. In the case of Htr-deficient SRI, the formation of SRI_{380} can be correlated with the appearance of one proton in the bulk medium per SRI_{380} formed (26), but at the same time the recovery of the initial state is slowed to about 30 s at pH 7 (27). Thus, a one-photon process could only drive proton translocation at very slow speed but a two-photon process might be efficient enough to be detected in intact cells by standard techniques.

Here we report the results of experiments with cells overproducing HtrI-free SRI by a factor of 50 (28). SRI is indeed shown to be active in proton translocation in a two-photon-driven process involving the two photocycle intermediates SRI_{380} and SRI_{520}.

MATERIALS AND METHODS

Bacterial Strains. *H. salinarium* strain Q6, used for transport experiments and cell membrane preparations, is a SRI-overproducing strain which has been constructed by transforming the SRI deletion strain HSN21 with the plasmid pEF198ΔC (28). Overproduction occurs by a factor of 50 as compared with the parent SRI wild-type strain HN5 (BR^-, HR^-) (K. Rumpel and D.O., unpublished work). HSN21 is derived from HN5 in exactly the same way as described for LSD3 (28). Mutant strain D76N is also a derivative of strain HSN21 and was obtained from G. Hübner (G. Hübner and D.O., unpublished work). Cells were grown as described (29).

Proton Translocation Experiments. Aliquots (15 ml) of the cell suspension were centrifuged for 10 min at 7000 × *g* and 15°C. The cells were suspended very gently in basal salt (medium without peptone) without sodium citrate and diluted to an OD_{578} of 0.5–0.7 (Spektralphotometer PM 6; Zeiss). Tetraphenylphosphonium (TPP^+, chloride salt, 100 mM in ethanol) was added to a final concentration of 250 μM and cells were preincubated for 1 hr.

The publication costs of this article were defrayed in part by page charge payment. This article must therefore be hereby marked "*advertisement*" in accordance with 18 U.S.C. §1734 solely to indicate this fact.

Abbreviations: SRI, sensory rhodopsin I; BR, bacteriorhodopsin; HR, halorhodopsin; TPP+, tetraphenylphosphonium.

*To whom reprint requests should be addressed.

The cell suspension (8 ml) was illuminated with either white or filtered light from one or two 900-W xenon lamps focused onto a 10-ml cuvette containing the cell suspension, which was thermostatted at 20°C. The pH was monitored with an electrode (Ingold, Steinbach/TS) which had the Ag/AgCl wire well shielded from incident light to minimize artifacts and was connected via the pH meter to a chart recorder and a personal computer. Initial rates of the pH changes upon illumination were taken as a measure of transport activity (30).

Neutral glass and cutoff filters were from Schott (Mainz, Germany). Interference filters varied from 30% to 70% transmission with a bandwidth of 15–20 nm. Action spectra were recorded in the presence of either orange or blue background light by irradiance through interference filters (see also legend to Fig. 2). Irradiance was measured with a ×40 Opto-Meter (United Detector Technology, Santa Monica, CA). Action (transported H^+/unit of photon flux) is displayed in Fig. 2 as relative action as a percentage of that at 520 nm or 380 nm.

Membrane Preparation. Cell growth and membrane preparation followed standard protocols (29) with minor changes. Cell lysis was induced by dialysis against buffer (10 mM $MgCl_2$/250 mM NaCl/10 mM sodium phosphate, pH 6.0, 4°C) which was also used in the following washing steps and for the sucrose gradient solutions. Centrifugation gave a single broad band on sucrose density gradients (25–45%, wt/wt) of apparent buoyant density around 1.18 g/cm^3.

Flash Photolysis. Difference spectra were recorded with a homemade flash photolysis spectrophotometer with a time resolution of 130 μs (31).

RESULTS

Proton Translocation Activity. Trace a in Fig. 1 shows pH changes in a cell suspension supplemented with 250 μM TPP^+ and illuminated with white light. At pH 6.7 an acidification of the medium by 0.1 pH unit can be measured. This must be due to active light-driven proton translocation because the presence of TPP^+ decouples any ion pump—except a proton pump—from proton movements in these membranes (32), and the addition of protonophores reduces the signal to the level of the light artifact (Fig. 1, trace c).

The pH changes increase with irradiance, and a plot of the inverse irradiance versus the inverse signal allows extrapolation to saturating intensities. This value, together with the SRI content of the cell suspension obtained from the maximal bleaching amplitude at 590 nm, yields a specific activity of about 12 H^+ per SRI per min, if we assume an extinction coefficient of $\varepsilon_{590} = 54{,}000\ M^{-1}\cdot cm^{-1}$ (8). This equals only 4% of the maximal turnover number of BR (280 H^+ per BR per min) measured under the same conditions (30).

A Two-Photon Reaction. Neither orange light (>475 nm) nor blue light (386 ± 10 nm) alone causes pH changes in the suspension above the level of artifacts (Fig. 1, trace b). Only simultaneous illumination with both light qualities leads to acidification of the suspension. This clearly indicates a two-photon reaction sequence as the basis of proton translocation.

pH Dependence. Acidification of the cell suspension is observed in the pH range of 5.7–8, with optimum activity around pH 7 (Fig. 1 *Inset*). Above pH 8 no signal can be detected. Surprisingly, below pH 5.7 the signal is inverted; i.e., an alkalinization of the suspension occurs upon illumination. Alkalinization at pH 4.8 is also based on a two-photon reaction analogous to the acidification process (data not shown).

Due to the low sensitivity of the electrode at acidic pH, quantitative evaluation of this effect is difficult and leads to a large experimental error. Nevertheless, the data suggest that the magnitudes of maximal acidification and alkalinization are about the same. Addition of the protonophore dinitrophenol (50 μM) reduces the signal of alkalinization to the level of the light artifact. Thus SRI can act at higher pH as an outwardly directed proton pump and at lower pH as an inwardly directed proton pump.

Action Spectra. To identify the light-absorbing species in the transport process, action spectra were determined in the presence of orange or blue background light (Fig. 2). The action spectrum of the blue light-absorbing species coincides reasonably well with the absorption spectrum of the known SRI_{380} intermediate of the photocycle of SRI (6). The orange

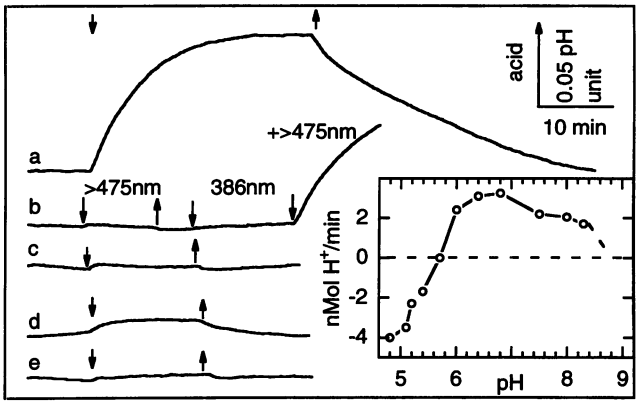

FIG. 1. Light-induced pH changes in a cell suspension at pH 6.7. Onset and offset of illumination are indicated by downward and upward arrows, respectively. Trace a, illumination of Q6 cells with white light (150 mW/cm^2); trace b, illumination with orange light (100 mW/cm^2, 475-nm cutoff filter) and/or blue light (60 mW/cm^2, 386-nm interference filter); trace c, signal under conditions as in trace a but after addition of the protonophore 3-carbonylcyanide-3-chlorophenylhydrazone (50 μM); trace d, illumination with white light of cells expressing mutant SRI D76N; trace e, as in trace d but after addition of 50 μM 3-carbonylcyanide-3-chlorophenylhydrazone. (*Inset*) pH dependence of proton transport activity. The pH of the cell suspensions was adjusted with microliter amounts of diluted HCl or NaOH. pH changes in white light were calibrated by addition of known amounts of 10 mM HCl, and initial rates were plotted against pH.

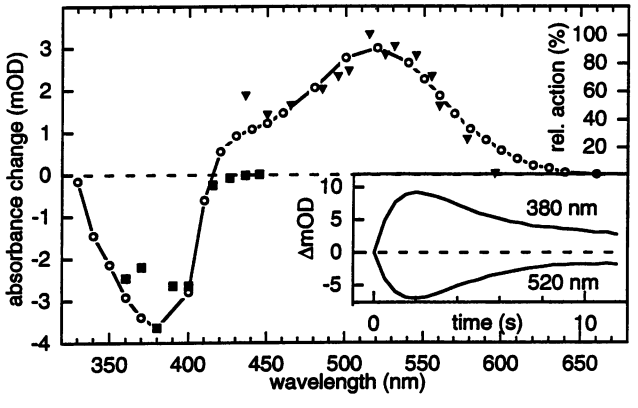

FIG. 2. Comparison of the action spectrum of proton transport in intact cells and light-induced difference spectra of cell membranes. The action spectrum in the blue region (■) was measured in the presence of orange background light (100 mW/cm^2, 475-nm cutoff filter). The action in the green region (▼) was recorded in the presence of blue background light (60 mW/cm^2, 360 ± 15-nm interference filter). The blue part is shown inverted to stress congruence with the difference spectrum (○). mOD, OD milliunits. (*Inset*) Absorbance changes at 380 nm and 520 nm of a SRI membrane suspension (4 M NaCl/10 mM sodium phosphate, pH 7.5) in the white measuring light (2 mW/cm^2 in the range 300–650 nm) of the spectrophotometer. The difference spectrum represents absorbance changes occurring between 2 s and 8 s. The difference spectrum between the onset of the measuring light (time zero) and 2 s is that between the initial state and SRI_{380} (data not shown).

light-absorbing species, on the other hand, is apparently not identical to the initial state SRI_{590} or SRI_{550} (see below), but instead the action spectrum identifies a species absorbing around 520 nm. This species may be identical to SRI_{520}, the photoproduct of SRI_{380}.

SRI overproduced in Q6 cells is not complexed by its transducer HtrI, and the absorbance maximum of the initial state is dependent on pH in the physiological range of pH 6–8. Difference spectra of SRI-overproducing cells after a 590-nm laser flash were recorded as a function of pH and are shown in Fig. 3. A shift of the absorption maximum of SRI from 590 nm at low pH to 550 nm at high pH with an apparent pK of 7.4 is seen. The lowest value in the difference maxima in Fig. 3 (550 nm) is clearly different from the maximum of about 520 nm in the action spectrum of Fig. 2 and excludes an initial-state SRI as the active species in proton translocation. This constitutes the unique situation of a two-photon process between intermediates of the photocycle of a retinal protein causing ion translocation.

Accumulation of the Intermediates SRI_{380} and SRI_{520} in White Light. In constant white light SRI is converted into a photostationary mixture of initial state and various photoproducts. Fig. 2 *Inset* shows the time course of this process in a suspension at pH 7.5. At this pH the dark state consists of a mixture of SRI_{550} and SRI_{590}, both of which contribute to the formation of SRI_{380} (see Fig. 3). Initially the dark state of SRI is depleted, as seen by the decrease in absorption at 520 nm, and the photoproduct SRI_{380} rises in concentration. After reaching a peak at about 2 s, the SRI_{380} concentration decreases while the absorption at 520 nm increases to a steady-state level. This is not caused by the re-formation of SRI_{590} or SRI_{550}. The difference spectrum between the mixture at 2 s and 8 s in Fig. 2 (○) identifies SRI_{520} as the species which is formed. The underlying kinetic scheme of the overall process must consist of a fast photochemical formation of SRI_{380} followed by a slower equilibration with SRI_{520} to a photosteady state (see also below).

At pH 4.8 (Fig. 4) only SRI_{590} exists and the evolution of a photosteady state is different. In the first second, a fast conversion of a part of the dark-state SRI_{590} to SRI_{380} is seen. In parallel, a slower bleaching of a dark state occurs with a concomittant absorbance increase at 500 nm. If the actinic light is cut off below 450 nm (cutoff filter GG455; Schott), a bleaching of the dark state yet no absorbance increase at 500 nm is observed (data not shown). This proves that the developing absorption at 500 nm in white light is due to the photochemical reaction of SRI_{380} and is caused by the SRI_{520} intermediate. Obviously the photochemical reaction of a dark state is limiting while that of SRI_{380} is faster, leading to the observed difference spectrum. SRI_{520} formation is connected to the slowly bleaching dark state.

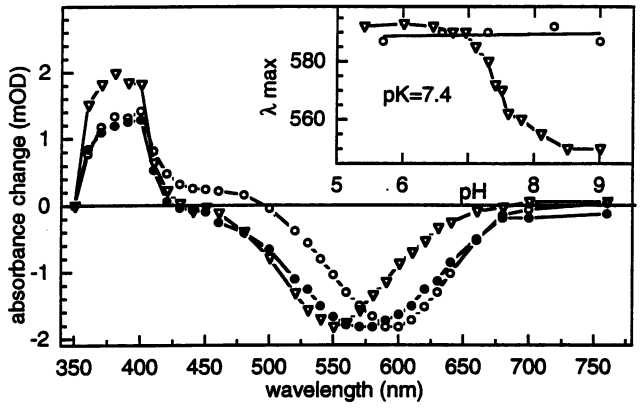

FIG. 3. pH dependence of light-induced difference spectra in intact cells. Cells were suspended in basal salt with 10 mM Mops and illuminated with laser light (590 nm, 50-Hz repetition rate, 3 mJ per pulse). The pH was adjusted with microliter amounts of dilated HCl or NaOH. Difference spectra are shown at pH 6 (○), pH 7.5 (●), and pH 8.5 (▽). mOD, OD milliunits. (*Inset*) pH dependence of the difference absorbance minimum of cells expressing wild-type SRI (▽) or mutant SRI D76N (○).

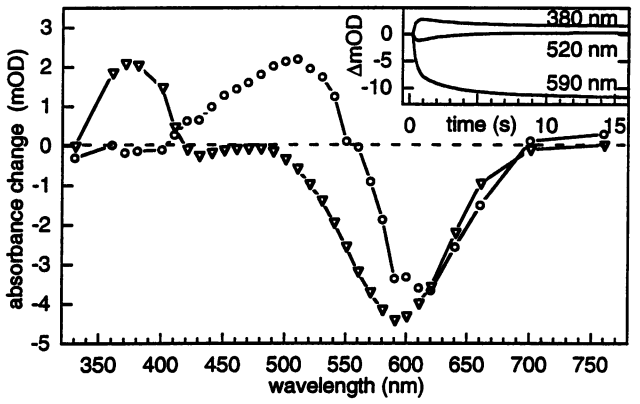

FIG. 4. Evolution of a photosteady state at pH 4.8. Measuring conditions were as in Fig. 2, with pH adjusted to 4.8. The difference spectra correspond to 0.4–0 s (▽) and 15–1.4 s (○). mOD, OD milliunits. (*Inset*) Absorbance changes at the indicated wavelength.

Photochemical Reaction of SRI_{520}. The action spectrum of proton transport identifies SRI_{520} as the photochemically active species. We analyzed the product of this reaction in the same setup as described above. In the measuring white light beam of the spectrophotometer, SRI_{380} and SRI_{520} accumulate at pH 8 (see Fig. 2). This allows measurement of the photoreaction of SRI_{520} after excitation with a laser flash (520 nm). Within the time resolution of the spectrophotometer (130 μs), SRI_{380} is formed from SRI_{520} (Fig. 5). This represents an unknown reaction of this intermediate of the SRI photocycle. Under continuous illumination SRI is converted to a mixture of photochemical products which equilibrate in a two-photon process. This forms the basis for active ion transport. However, in neither of the two transport processes, acidification or alkalinization, does a molecular mechanistic explanation seem obvious (see *Discussion*).

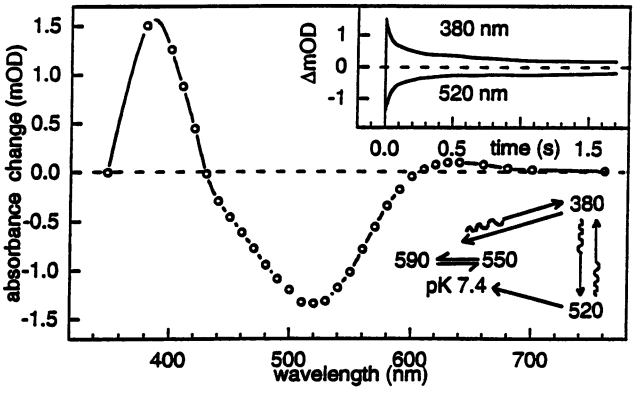

FIG. 5. Photochemical reaction of SRI_{520}. A membrane suspension of wild-type SRI in 4 M NaCl/10 mM sodium phosphate, pH 8, was illuminated for 1 min with white measuring light of the spectrophotometer to allow accumulation of SRI_{520} in a photostationary equilibrium (compare with Fig. 2). The photochemical reaction was induced by a nanosecond laser flash (520 nm, 2 mJ). The first difference spectrum can be recorded at 130 μs and is identical to the one shown (1.2 ms) except for a laser artifact. mOD, OD milliunits. (*Upper Inset*) Time course of absorbance changes at 380 nm and 520 nm. (*Lower Inset*) Simplified scheme of the SRI photocycle including the pH-dependent initial-state absorption maximum and the SRI_{520}-to-SRI_{380} photoreaction.

Mutation of the Potential Proton Acceptor Side Chain of Asp-76. The pH-induced shift of the absorption maximum from 590 to 550 nm has an apparent pK of 7.4 in the case of transducer-free SRI but 8.5 in case of the SRI–HtrI complex. The mutated SRI D76N does not show the same pH dependence of the absorption maximum (Fig. 3 *Inset*).

The proton acceptor in the BR-M transition is Asp-85. The equivalent position 76 in SRI is also an aspartic acid. With the mutant SRI D76N (Asp-76 → Asn), a most intriguing question can be asked: is Asp-76 in SRI indeed the functional equivalent to Asp-85 in BR? The proton transport experiments show activities below 10% of wild type in both alkaline (Fig. 1, traces d and e) and acidic (data not shown) solutions. This shows that Asp-76 is necessary for proton transport in SRI and therefore performs a function similar to that of Asp-85 in BR.

DISCUSSION

We have shown that cells devoid of light-driven ion pumps but overproducing SRI by a factor of 50, when compared with the corresponding wild type, cause pH changes under illumination with white light. These changes were measured in the presence of TPP^+, which excludes the possibility that they are a secondary effect induced by activity of any other ion pump. Addition of uncouplers for proton gradients abolishes acidification as well as alkalinization signals at the respective pH values, which proves that the primary pump process is proton translocation in either case. Thus we consider our results as proof that SRI is a proton pump with a pH-dependent vectoriality, a property which to our knowledge has not been found for any other proton-translocating system. From its maximal turnover number a rate-limiting thermal rate constant of about 4 s^{-1} can be estimated.

From Fig. 1, trace b, it is evident that induction of transport activity in SRI results from a two-photon process. An analogous phenomenon is found for proton translocation by the anion pump HR (33) and by the BR mutants D85N, D85T, and D85,96N (21).

Action spectroscopy in the presence of background light was used to identify the light-absorbing species in the acidification process. The photocycle intermediate SRI_{380} turns out to be the blue light-absorbing species. Its photochemical reaction is long known (6), leading back to the initial state via a SRI_{520} intermediate (7, 8). Surprisingly, the second species involved is not the initial-state SRI_{590} or SRI_{550} but rather the SRI_{520} intermediate. This requires both the accumulation of this intermediate under photostationary conditions as well as its photochemical activity. The accumulation is demonstrated by the experiment in Figs. 2 and 4, whereas flash photolysis experiments with SRI_{520} show that SRI_{380} is formed from SRI_{520} in <200 μs with no detectable intermediate. The possibility of a light-induced back reaction to the initial state followed by absorption of a second photon leading to reformation of SRI_{380} in a three-photon cycle can be excluded because the process of formation and subsequent photoreaction of SRI_{380} is time-resolved under the measuring conditions (compare rise and decay of the 380-nm trace in Fig. 2).

Under the conditions of high-intensity illumination applied in the proton translocation experiments, the photoprocess obviously outweighs the competing thermal decay of SRI_{520} and SRI_{380} to the initial-state SRI_{590}/SRI_{550}. These results lead to our proposal that proton translocation is driven by a secondary cycle involving photoinduced transitions between SRI_{380} and SRI_{520}, bypassing the initial state (Fig. 5 *Lower Inset*). The initial state has to be converted to the SRI_{380} intermediate only once to start this secondary cycle (neglecting those SR molecules that "escape" the secondary cycle by thermal decay of SRI_{380} or SRI_{520} to the initial state). Note that if this transition were limiting in the determination of the action spectrum the apparent maximum would tend to be red-shifted.

The unphotolyzed state of SRI shows a pH-induced shift of its absorbance maximum from 590 to 550 nm, which is not found for the mutant SRI D76N. This suggests that Asp-76 in SRI has a pK around 7.4 and causes an absorption maximum of 590 nm and 550 nm in its protonated and deprotonated state, respectively. A redshift induced by the absence of a negative charge in the vicinity of the protonated Schiff base is also found for BR when Asp-85 is neutralized by protonation (34) or replaced by an uncharged residue (35).

A detailed understanding of the molecular mechanism of proton translocation by SRI is impossible at this time. A tempting interpretation, in analogy to the mechanism of BR, would involve Asp-76 as carboxylate group for the outwardly directed proton translocation as a proton acceptor in the alkaline range. Inwardly directed proton translocation in the acidic range, where Asp-76 is protonated, could be similar to a mechanism assumed for the inverted proton translocation found for HR (33) and BR mutants lacking the proton-accepting carboxylate at residue 85 (21).

An obvious problem with this model is that the inversion point of vectoriality (pH 5.7) does not coincide with the pK of 7.4 for the SRI_{590}-to-SRI_{550} transition (Δ = 7.4–5.7). Part of the discrepancy might be resolved by assuming different efficiencies for the two processes. But since Δ = 1.7, efficiencies would have to differ by an unlikely factor of 50. A second possible explanation would be that the pK of Asp-76 might be lowered in the photocycle intermediates SRI_{380} and/or SRI_{520} compared with the value of 7.4 for the unphotolyzed state, which is not involved in the secondary pump cycle.

A third point to consider is the different evolution of the photostationary mixture and accumulation of SRI_{520} depending on pH. As can be seen from Figs. 2 and 4, SRI_{520} formation is limited by the SRI_{380} light reaction at pH 7.5, since it accumulates before being converted to SRI_{520}, but by the bleaching of the dark state with slow kinetics at pH 4.8. Vectoriality of translocation could be dependent on these kinetic differences and independent of the pK of Asp-76. It is then the result of complex kinetics and the specific experimental conditions—e.g., the ratio of blue to orange light used in the experiment.

Light-induced reactions of retinal proteins can be assumed to involve isomerization of the retinal. This presumably leads to an all-*trans* configuration in SRI_{520}, since SRI_{380} was shown by resonance Raman spectroscopy to contain a 13-*cis*-retinal (15). The proton translocation is then based on the light-induced transitions between the 13-*cis* and all-*trans* configuration. To yield outwardly directed proton translocation on the basis of the secondary cycle constituted by the SRI_{380}/SRI_{520} system, formation of SRI_{380} must be connected with proton release on the extracellular side, while proton uptake during SRI_{520} formation occurs from the cytoplasmic side. Therefore, the accessibility of the Schiff base must change, presumably due to a conformational change of the protein. This change and the *trans*-to-*cis* isomerization itself have both been called the "switch" in the discussion of the mechanism of BR (21, 36). To avoid confusion we suggest that the isomerization of retinal be called the "trigger" for the conformational change which constitutes the necessary switch to change the accessibility of the Schiff base. The two transitions are intrinsically connected to each other.

While reprotonation of the Schiff base after photochemical reaction of SRI_{380} is from the cytoplasmic side, it must be from the extracellular side after the blue light-induced M–BR backreaction which quenches proton translocation (37). This difference may be accounted for by assuming the kinetic independence of the proton transfer catalysis and the reprotonation switch. After retinal isomerization there would be a kinetic competition between the proton transfer to/from the

Schiff base and the change of its accessibility. The vectoriality of the proton translocation is then determined by the ratio of the rate constants of proton transfer (k_t) and reprotonation switch (k_s). The k_s/k_t ratio could be inverted for the two retinal proteins and, more specifically, for SRI it could be inverted going from high to low pH, resulting in the observed change in vectoriality. This general concept of the kinetic independence of proton transfer and change of accessibility of the Schiff base may be applied to all ion-translocating retinal proteins in order to yield a general understanding of the factors that determine vectoriality.

Another problem with the proposed analogy to the mechanism of proton translocation in BR and its mutants is that it would predict an inwardly directed proton translocation of SRI D76N (corresponding to BR D85N). This is found not for the mutant but for wild-type SRI at low pH, where Asp-76 is protonated. Since large conformational changes of the local structure are unlikely in this isomorphic substitution, we suggest that Asp-76 in its protonated state is required for the efficient catalysis of proton translocation. This could be due to the ability of a protonated carboxyl group to be part of a hydrogen-bond network and to very rapidly exchange protons with the bulk solution, in contrast to the carboxamide group.

Applying the idea of kinetic independence of proton transfer and reprotonation switch would predict that in the mutant SRI D76N, k_t would be smaller than k_s after the first light reaction ($k_s \gg k_t$) and larger after the second ($k_s \ll k_t$), or vice versa, leading to only a transient release of a proton on the extracellular or intracellular side, respectively.

Note. During review of this paper, Bogomolni *et al.* (38) have presented results partially different from ours. Further investigations are necessary to resolve the contradictions.

G. Hübner is acknowledged for providing the mutant strain SRI D76N. We thank J. Tittor and M. Rüdiger for critical comments and discussion of the manuscript.

1. Lanyi, J. K. (1993) *Biochim. Biophys. Acta* **1183,** 241–261.
2. Lanyi, J. K. (1993) in *The Biochemistry of Archea (Archaebacteria)*, eds. Kates, M., Kushner, D. J. & Matheson, A.T. (Elsevier, Amsterdam), pp. 189–207.
3. Oesterhelt, D. & Marwan, W. (1993) in *The Biochemistry of Archea (Archaebacteria)*, eds. Kates, M., Kushner, D. J. & Matheson, A.T. (Elsevier, Amsterdam), pp. 173–187.
4. Spudich, J. L. (1993) *J. Bacteriol.* **175,** 7755–7761.
5. Spudich, J. (1983) *Biophys. J.* **43,** 243–246.
6. Bogomolni, R. A. & Spudich, J. L. (1982) *Proc. Natl. Acad. Sci. USA* **79,** 6250–6254.
7. Tomioka, H., Kamo, N., Kamo, N., Takahashi, T. & Kobatake, Y. (1984) *Biochem. Biophys. Res. Commun.* **123,** 989–994.
8. Spudich, J. L. & Bogomolni, R. A. (1984) *Nature (London)* **312,** 509–513.
9. Blanck, A., Oesterhelt, D., Ferrando, E., Schegk, E. S. & Lottspeich, F. (1989) *EMBO J.* **8,** 3963–3971.
10. Khorana, H. G., Gerber, G. E., Herlihy, W. C., Gray, C. P., Anderegg, R. J., Nihei, K. & Bieman, K. (1979) *Proc. Natl. Acad. Sci. USA* **76,** 5046–5050.
11. Blanck, A. & Oesterhelt, D. (1987) *EMBO J.* **6,** 265–273.
12. Henderson, R., Baldwin, J. M., Ceska, T. A., Zemlin, F., Beckmann, E. & Downing, K. H. (1990) *J. Mol. Biol.* **213,** 899–929.
13. Havelka, W. A., Henderson, R., Heymann, J. A. W. & Oesterhelt, D. (1993) *J. Mol. Biol.* **234,** 837–846.
14. Fodor, S. P. A., Gebhard, R., Lugtenburg, J., Bogomolni, R. A. & Mathies, R. A. (1989) *J. Biol. Chem.* **264,** 18280–18283.
15. Haupts, U., Eisfeld, W., Stockburger, M. & Oesterhelt, D. (1994) *FEBS Lett.* **356,** 25–29
16. Butt, H. J., Fendler, K., Bamberg, E., Tittor, J. & Oesterhelt, D. (1989) *EMBO J.* **8,** 1657–1663.
17. Braiman, M. S., Mogi, T., Marti, T., Stern, L. J., Khorana, H. G. & Rothschild, K. J. (1988) *Biochemistry* **27,** 8516–8520.
18. Gerwert, K., Souvignier, G. & Hess, B. (1990) *Proc. Natl. Acad. Sci. USA* **87,** 9774–9778.
19. Bousché, O., Spudich, E. N., Spudich, J. L. & Rothschild, K. J. (1991) *Biochemistry* **30,** 5395–5400.
20. Rath, P., Olson, K. D., Spudich, J. L. & Rothschild, K. J. (1994) *Biochemistry* **33,** 5600–5606.
21. Tittor, J., Schweiger, U., Oesterhelt, D. & Bamberg, E. (1994) *Biophys. J.* **67,** 1682–1690.
22. Ehrlich, B. E., Schen, C. R. & Spudich, J. L. (1984) *J. Membr. Biol.* **82,** 89–94.
23. Yao, V. J. & Spudich, J. L. (1992) *Proc. Natl. Acad. Sci. USA* **89,** 11915–11919.
24. Ferrando-May, E., Krah, M., Marwan, W. & Oesterhelt, D. (1993) *EMBO J.* **12,** 2999–3005.
25. Krah, M., Marwan, W., Verméglio, A. & Oesterhelt, D. (1994) *EMBO J.* **13,** 2150–2155.
26. Olson, K. D. & Spudich, J. L. (1993) *Biophys. J.* **65,** 2578–2585.
27. Spudich, E. N. & Spudich, J. L. (1993) *J. Biol. Chem.* **268,** 16095–16097.
28. Ferrando-May, E., Brustmann, B. & Oesterhelt, D. (1993) *Mol. Microbiol.* **9,** 943–953.
29. Oesterhelt, D. & Stoeckenius, W. (1974) *Methods Enzymol.* **31,** 667–678.
30. Oesterhelt, D. (1982) *Methods Enzymol.* **31,** 10–17.
31. Uhl, R., Meyer, B. & Desel, H. (1985) *J. Biochem. Biophys. Methods* **10,** 35–48.
32. Wagner, G., Oesterhelt, D., Krippahl, G. & Lanyi, J. K. (1981) *FEBS Lett.* **131,** 341–345.
33. Bamberg, E., Tittor, J. & Oesterhelt, D. (1993) *Proc. Natl. Acad. Sci. USA* **90,** 639–643.
34. Fischer, U. & Oesterhelt, D. (1979) *Biophys. J.* **28,** 211–230.
35. Turner, G. J., Mierke, L. J. W., Thorgeirsson, T. E., Kliger, D. S., Betlach, M. C. & Stroud, R. M. (1993) *Biochemistry* **32,** 1332–1337.
36. Fodor, S. T. P., Ames, J. B., Gebhard, R., van den Berg, E. M. M., Stoeckenius, W., Lugtenburg, J. & Mathies, R. A. (1989) *Biochemistry* **27,** 7097–7101.
37. Ormos, P., Dancshazy, Z. & Karvaly, B. (1978) *Biochim. Biophys. Acta* **503,** 304–315.
38. Bogomolni, R. A., Stoekenius, W., Szundi, I., Perozo, E., Olson, K. D. & Spudich, J. L. (1994) *Proc. Natl. Acad. Sci. USA* **91,** 10188–10192.